SAND2021-6266C

Sandia National Laboratories

Towards Higher-Order Validation Methodology for Actuator Line LES Near-Wake Predictions using Nacelle-Mounted LiDAR Measurements

Presented by:

Kenneth Brown, Thomas Herges, Lawrence Cheung, Myra Blaylock, Alan Hsieh, and David Maniaci

Wind Energy Technologies / Thermal-Fluid Science & Engineering

Sandia National Laboratories

May 27, 2021

U.S. DEPARTMENT OF ENERGY NNSA

SAND Number: SAND2021-?????

Introduction

State-of-the art LES wake simulations have been validated for time-averaged quantities

- High Reynolds number examples: Jimenez *et al.* [1], Troldborg *et al.* [2], Porté-Agel et al. [3], Machefaux et al. [4], Moriarty *et al.* [5], and Doubrawa et al. [6]

However, there has been relatively little validation of higher-order wake dynamics

- Andersen *et al.* [7] – POD analysis showed streamwise planar PIV measurements in the near wake which had more gradual energy roll-off with mode number than LES simulations

Current objective: prove techniques for field validation of higher-order LES dynamics

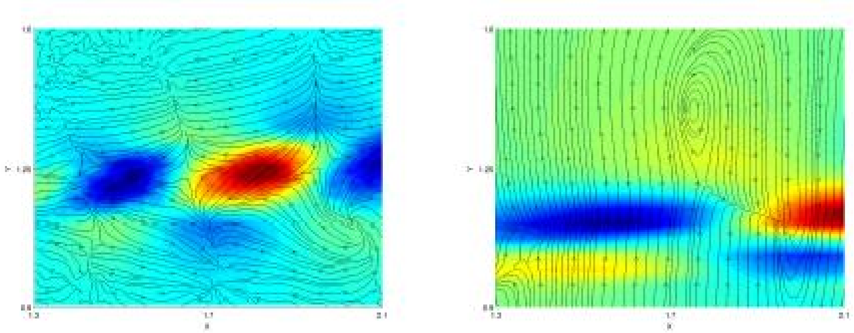

POD mode 2 from Andersen *et al.* [7]

Field Validation Case

Facility

- Scaled Wind Farm Technology (SWiFT) facility in Lubbock, Texas, USA
  - Characterization of the atmospheric conditions in [8], recent benchmarking activities given in [6]

Boundary Conditions

- Simulation B.C.'s derive from time-averaged measurements over six 10-minute intervals by the upstream met tower in a stable, night-time ABL

Lidar

- Continuous-wave DTU SpinnerLidar [9] rear-mounted on WTGa1
- A rosette pattern is completed in 2 s and consists of 984 measurement locations taken at locations between 0.5 – 5D downstream
- Lidar probe length results in spatial averaging of flow and also implies a degree of temporal anti-aliasing [10]
- In this study, we assume the lidar remains directed straight downstream as the turbine yaws

Turbine:

$\omega_{rotor} = 43.6$ rpm
$\gamma_{rotor} = 9.1°$

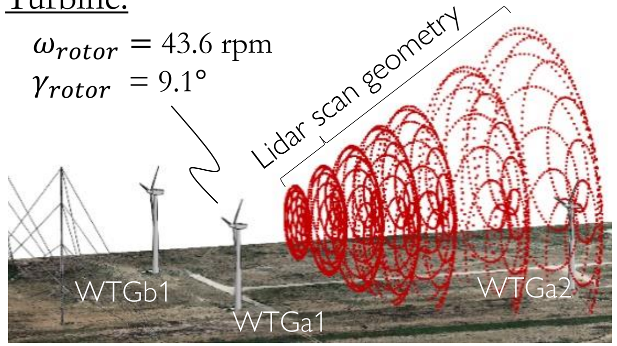

Flow:

$U_{hub} = 9.28$ m/s
$TI_{hub} = 5.93\%$
$\alpha = 0.42$

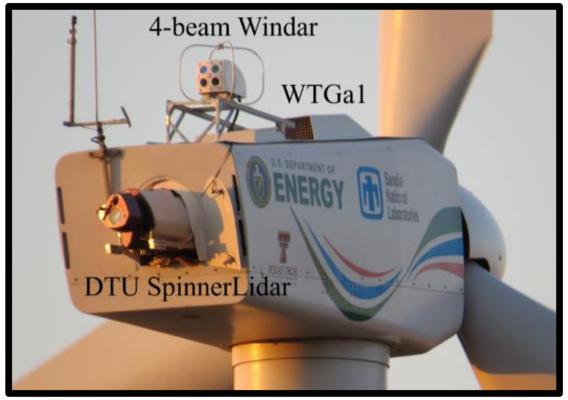

(Images from [6])

Measurement Errors from CW Nacelle-Mounted Lidar

Three primary sources of measurement error*:

1. Directional bias (due to a single, non-axial line-of-sight pointing direction)
2. Spatial averaging of inhomogeneous flow over the probe beamwise length
3. Instrument noise

*sources of error that may be of secondary importance include motion of the lidar beam during data capture, spatial interpolation of irregular scan patterns, temporal delays between scan positions, and instrument bias/solid-body interference

Simley *et al.* [2014]

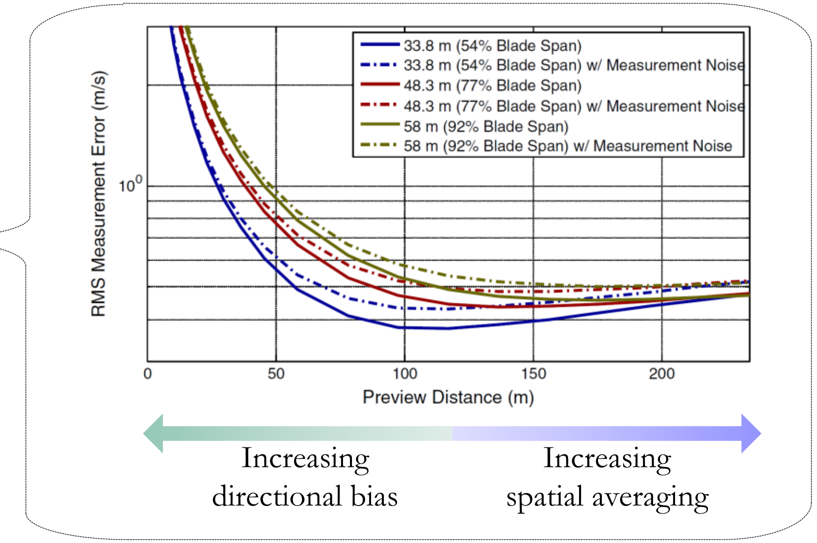

Existing literature investigating errors from virtual nacelle-mounted SpinnerLidars (or ZephIR lidars):

Ref.	Authors	*Lidar Setup* Configuration	*Lidar Setup* Type	*Simulation Setup* Type	*Simulation Setup* Code	*Simulation Setup* ABL Stability	*Simulation Setup* Turbine	*Simulation Setup* Yaw	*Quantities of Interest* Wake Position	*Quantities of Interest* Velocity	*Quantities of Interest* Turbulence	*Quantities of Interest* Spectra	*Quantities of Interest* Spatial POD
[11]	Simley *et al.* [2014]	Forward-facing	ZephIR	Stochastic turbulence field	TurbSim	S/N/U	NREL 5 MW	0°	N/A	✓			
[12]	Churchfield *et al.* [2016]	Rear-facing	SpinnerLidar	Actuator Line LES	SOWFA	S/N/U	Vestas 225 kW	0° - 40°	✓	✓			
[13]	Forsting *et al.* [2017]	Rear-facing	ZephIR	Actuator Line LES	EllipSys3D	Not specified	Siemens 2.3 MW	0°		✓			
[14]	Kelley *et al.* [2018]	Rear-facing	SpinnerLidar	Actuator Line LES	SOWFA	S	Vestas 225 kW	0°		✓			
[15]	Sekar *et al.* [2020]	Forward-facing	SpinnerLidar	Actuator Line LES	PALM	U	NREL 5 MW	0°	N/A	✓	✓	✓	
[16]	Brown *et al.* [2020]	Rear-facing	SpinnerLidar	Actuator Line LES	Nalu-Wind	N	Vestas 225 kW	0°			✓	✓	✓

Forward-facing cases do not include effects of inhomogeneities in the wake

Only [16] considers higher-order wake quantities, though these were for a neutral ABL inflow

Computational Setup

LES Domain

- Simulations use the multi-physics, massively parallel LES code Nalu-Wind, part of the ExaWind code suite [17]
  - One-equation, constant coefficient, turbulent kinetic energy (TKE) model
  - Actuator line model ($\varepsilon = 0.9$)
  - Coupled dynamic response of the wind turbines is performed through the OpenFAST software suite [18]
- Simulation time: 3600 s (i.e., >1300 independent flow realizations based on wake integral timescales)

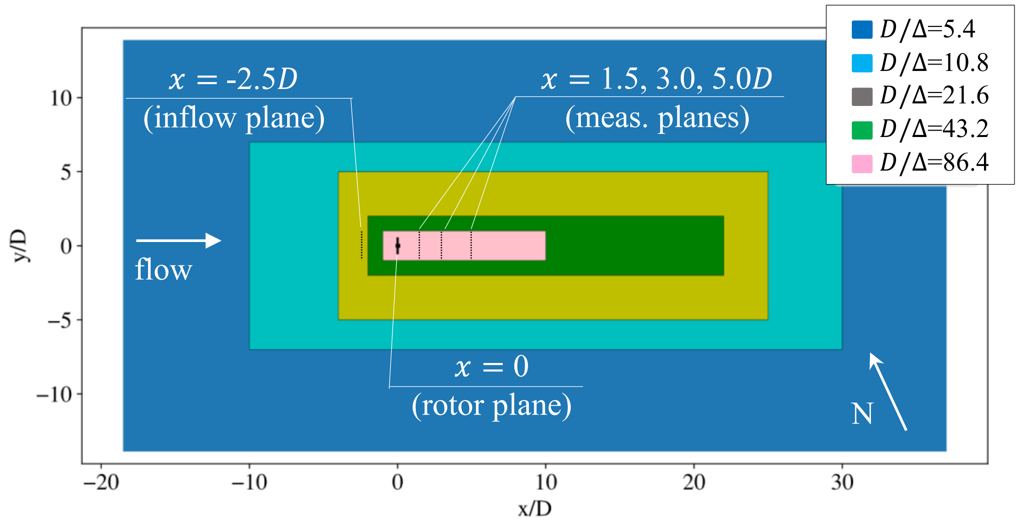

Flow Sampling

- Planar
  - Cross-stream sampling planes reported at 1.5D, 3D, and 5D downstream of WTGa1
- Virtual Lidar
  - Flowfield is sampled along radial vectors emanating from the mounted lidar position that scans the 984-point rosette pattern
  - Lidar is represented as an infinitely thin beam based on the small transverse dimension of the beam compared to the beam-wise length of its sampling volume
  - Truncated window probe volume weighting [19] is applied along each vector to obtain results corresponding to the desired focus distances
  - For this work, the lidar line-of-sight velocity was projection-corrected to the streamwise direction, and the camber of the lidar arc was neglected
  - Instrument noise is not considered here (similarly, see Fuertes and Porte-Agel, [20])

Results – Flow Structure

Method (proper orthogonal decomposition, POD):

- Space-only formulation (Sirovich, [21]) applied to cross-stream planes (a.k.a. – *slice* POD from Glauser and George, [22])
- Only streamwise component of TKE considered
- All cases are converged by at least 1800 s, where convergence is defined when $E(N)$<0.02 (see convergence criteria of Newman *et al.* [23])

Analysis:

- At 1.5D, most of the turbulent energy is at the shear layer, and the lidar successfully captures the progressively more complex character of the planar mode shapes as mode number increases.
- At 3.0 and 5.0D, mode shapes are qualitatively different between the planar and lidar starting at modes 3 - 4 as volume averaging and the coarse resolution of the scan pattern work to smooth over finer fluctuations in the wake.

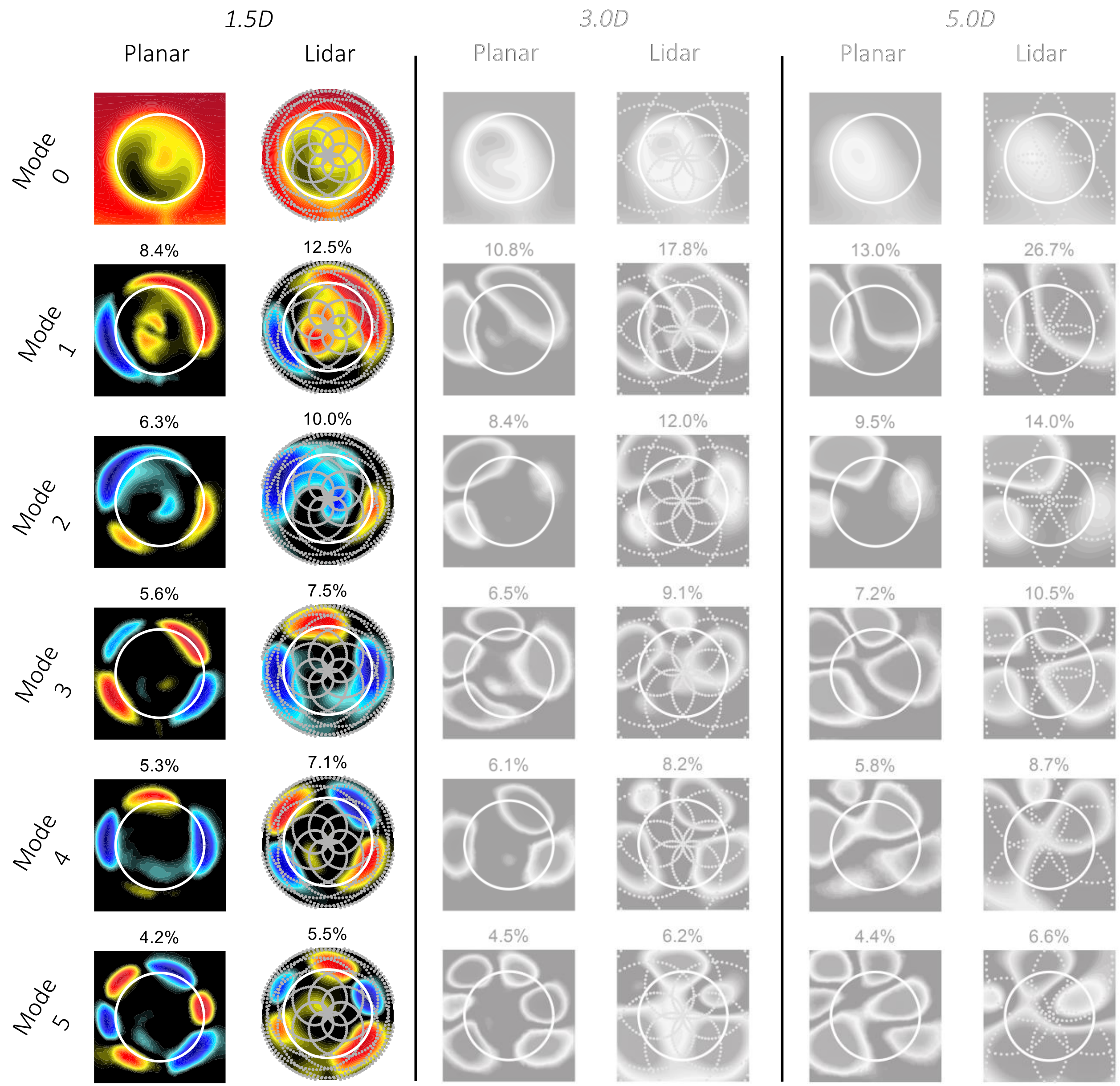

Results – Flow Structure

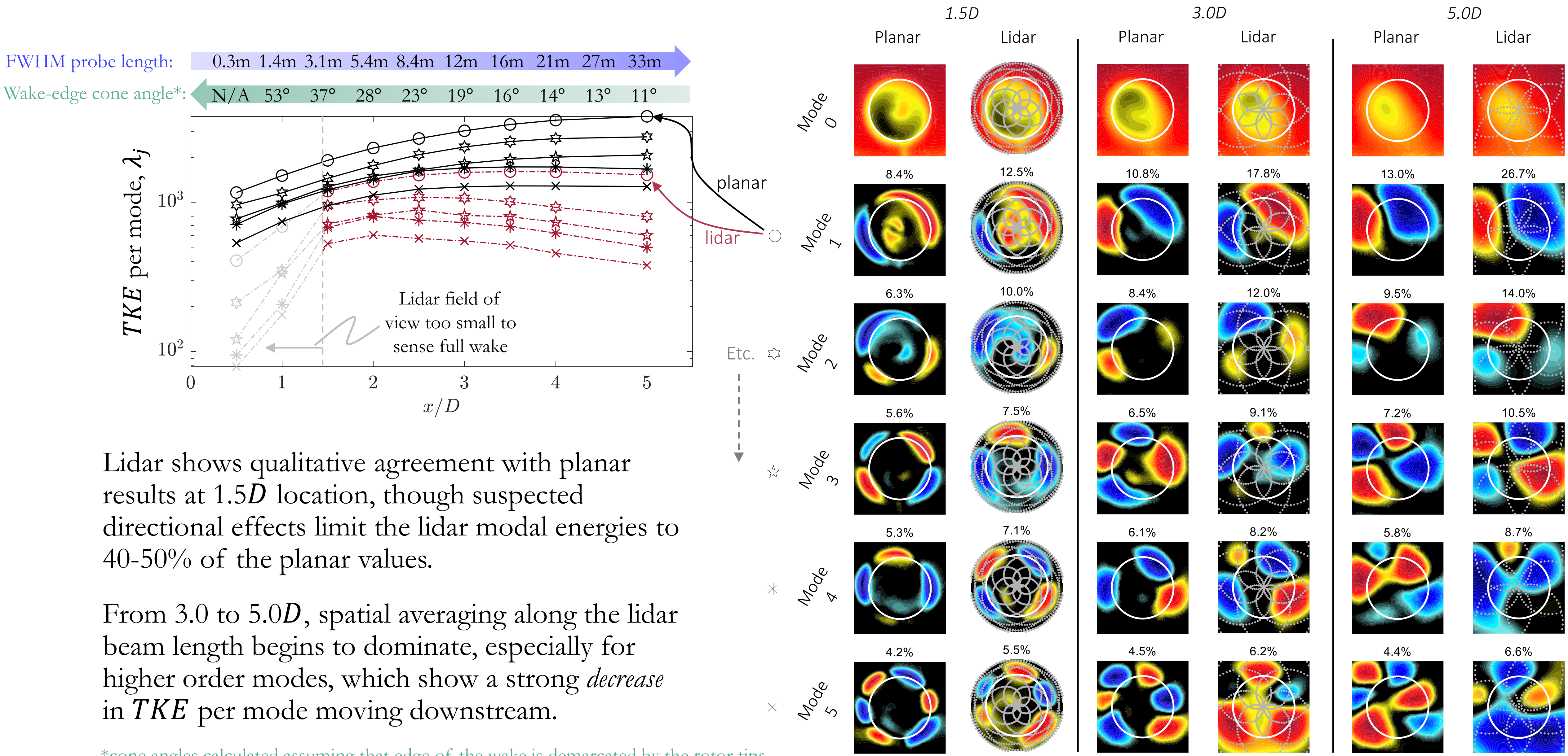

Lidar shows qualitative agreement with planar results at 1.5D location, though suspected directional effects limit the lidar modal energies to 40-50% of the planar values.

From 3.0 to 5.0D, spatial averaging along the lidar beam length begins to dominate, especially for higher order modes, which show a strong *decrease* in TKE per mode moving downstream.

*cone angles calculated assuming that edge of the wake is demarcated by the rotor tips

Results – Flow Spectra

One-dimensional spectra, S_{UU}, are calculated versus frequency, f

- Welch's method is applied with the Hanning window and an overlap of 50% for a total of 74 blocks
- Gray plots indicate uncorrected lidar data; the correction comes from Angelou *et al.* [24]

x = 1.5D

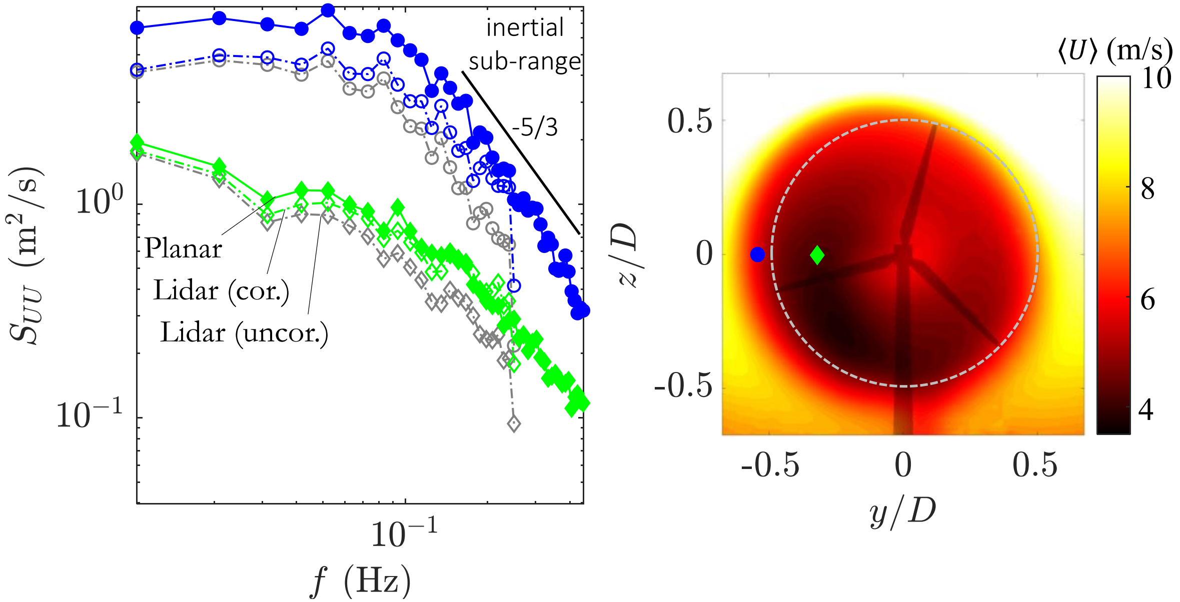

Without correction, the lidar spectra are attenuated at higher f due to the spatial averaging of finer turbulence structures within the probe volume.

Corrected lidar data at inboard location follow planar data and Kolmogorov -5/3 scaling albeit with some deviation near the Nyquist frequency due to aliasing. Corrected data at outboard location are biased due to strong directional effects.

Results – Flow Spectra

One-dimensional pre-multiplied spectra, $f * S_{UU}$, are calculated versus frequency, f

- Welch's method is applied with the Hanning window and an overlap of 50% for a total of 74 blocks
- Corrected data only shown below; the correction comes from Angelou *et al.* [24]

x = 1.5D

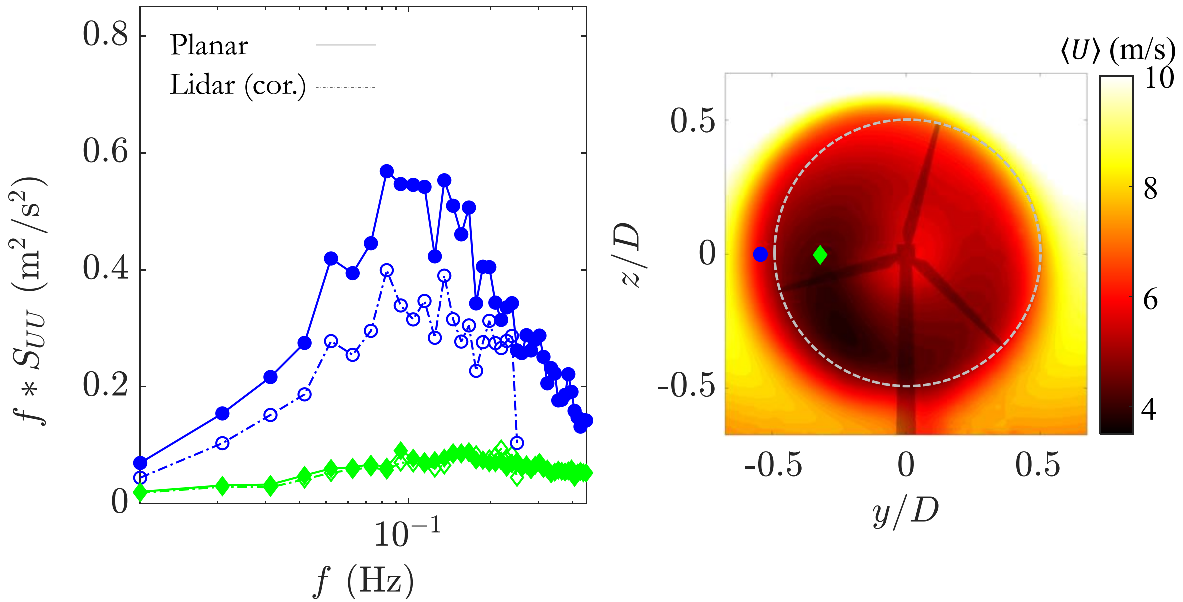

At 1.5D, the lidar captures well the most energetic scales for the inboard location but underestimates those of the outboard location by ~0.2 m^2/s^2.

Results – Flow Spectra

One-dimensional pre-multiplied spectra, $f * S_{UU}$, are calculated versus frequency, f

- Welch's method is applied with the Hanning window and an overlap of 50% for a total of 74 blocks
- Corrected data only shown below; the correction comes from Angelou *et al.* [24]

x = 3.0*D*

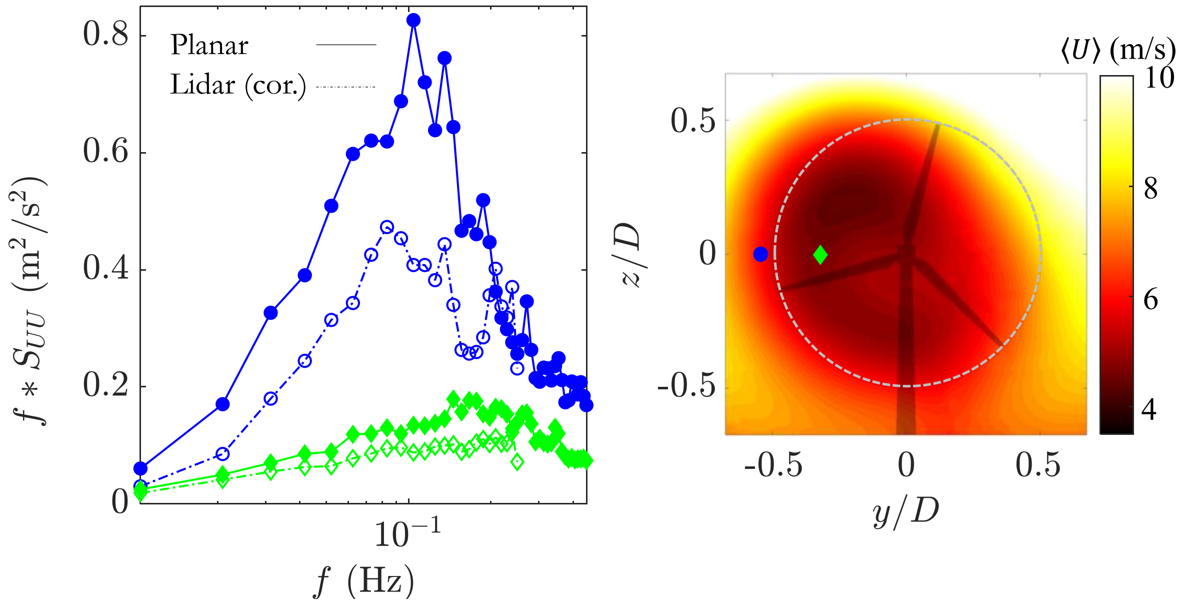

At 3.0D (and 5.0D), the correction is not reliable at neither inboard nor outboard locations.

↳ The correction magnitude at 3.0D is already very large (i.e., as much as 92% of the corrected value), so small errors in the correction model translate to large errors in the corrected spectra.

Conclusions

Nacelle-mounted, continuous-wave lidar can qualitatively reproduce large-scale mode structures compared to the full planar simulation results in the near-field wake (i.e., $x \cong 1.5D$) including dipole-, quadrupole-, and hexapole-type modes.

Initial attempts at correction of the higher-frequency turbulence spectral content for volume-averaging attenuation using the transfer function of Angelou *et al.* [24] were successful at inboard locations for $x = 1.5D$ though not at outboard locations near the shear layer or further downstream where directional effects and a large correction magnitude, respectively, were problematic.

Results of this work aid the design of experiments for validation of higher-order wake dynamics in high-fidelity models.

- The need to adequately resolve fine flow fluctuations limits the maximum usable range of the lidar measurements to $x < 3.0D$ because the smoothing that stems from probe-volume averaging reduces the accuracy of estimates of spatial modes and turbulence spectra at longer ranges.
- At the shorter ranges, the lidar's reconstruction of modes and spectra becomes inaccurate near the shear layer because of its inability to distinguish between Cartesian velocity components.

Future Work

Further computational studies

- Minimize directional bias by calculating three-component velocities from clusters of scan positions
- Perform the above analyses in the meandering frame of reference
- Perform analysis with dynamic mode decomposition

Full validation analysis

- Use measured data to validate wake dynamics of LES code Nalu-Wind for stable atmospheric boundary layer
  - Initial results indicate that the wake curl of the simulation is stronger than observed in the field

Thank you!

Sandia National Laboratories is a multimission laboratory managed and operated by National Technology & Engineering Solutions of Sandia, LLC, a wholly owned subsidiary of Honeywell International Inc., for the U.S. Department of Energy's National Nuclear Security Administration under contract DE-NA0003525.

Sandia National Laboratories

References

1. **Jimenez, A., et al.,** *Large-eddy simulation of spectral coherence in a wind turbine wake.* Environmental Research Letters, 2008. **3**(1): p. 015004.
2. **Troldborg, Niels.** "Actuator line modeling of wind turbine wakes." (2009).
3. **Porté-Agel, Fernando, et al.** "Large-eddy simulation of atmospheric boundary layer flow through wind turbines and wind farms." *Journal of Wind Engineering and Industrial Aerodynamics* 99.4 (2011): 154-168.
4. **Machefaux, Ewan, et al.** "Single wake meandering, advection and expansion-An analysis using an adapted pulsed lidar and CFD LES-ACL simulations." *European Wind Energy Conference & Exhibition 2013*. European Wind Energy Association (EWEA), 2013.
5. **Moriarty, Patrick, et al.** "IEA-task 31 wakebench: Towards a protocol for wind farm flow model evaluation. part 2: Wind farm wake models." Journal of Physics: Conference Series. Vol. 524. No. 1. IOP Publishing, 2014.
6. **Doubrawa, P., et al.,** *Multimodel validation of single wakes in neutral and stratified atmospheric conditions.* Wind Energy, 2020.
7. **Andersen, S.J., et al.** *Comparison between PIV measurements and computations of the near-wake of an actuator disc*. in *Journal of Physics: Conference Series*. 2014. IOP Publishing. **524** 012173.
8. **Kelley, C.L. and B.L. Ennis**, *SWiFT site atmospheric characterization.* 2016, Sandia National Lab.(SNL-NM), Albuquerque, NM (United States).
9. **Mikkelsen, T., et al.,** *A spinner-integrated wind lidar for enhanced wind turbine control.* Wind Energy, 2013. **16**(4): p. 625-643.
10. **Citriniti, J.H. and W.K. George**, *Reconstruction of the global velocity field in the axisymmetric mixing layer utilizing the proper orthogonal decomposition.* Journal of Fluid Mechanics, 2000. **418**: p. 137-166.
11. **Simley, Eric, et al.** "Analysis of light detection and ranging wind speed measurements for wind turbine control." Wind Energy 17.3 (2014): 413-433.
12. **Churchfield, M., et al.** "Using high-fidelity computational fluid dynamics to help design a wind turbine wake measurement experiment." Journal of Physics: Conference Series. Vol. 753. No. 3. IOP Publishing, 2016.
13. **Forsting, AR Meyer, Niels Troldborg, and Antoine Borraccino**. "Modelling lidar volume-averaging and its significance to wind turbine wake measurements." Journal of Physics: Conference Series. Vol. 854. No. 1. IOP Publishing, 2017.
14. **Kelley, Christopher Lee, et al**. "Wind turbine aerodynamic measurements using a scanning lidar." Journal of Physics: Conference Series. Vol. 1037. No. 5. IOP Publishing, 2018.
15. **Sekar, Anantha Padmanabhan Kidambi, et al.** "How much flow information can a turbine-mounted lidar capture?." Journal of Physics: Conference Series. Vol. 1618. No. 3. IOP Publishing, 2020.
16. **Brown, Kenneth, et al.** "Representation of coherent structures and turbulence spectra from a virtual SpinnerLidar for future LES wake validation." Journal of Physics: Conference Series. Vol. 1618. No. 6. IOP Publishing, 2020.
17. **Domino, S.,** *Sierra low mach module: Nalu theory manual 1.0*. SAND2015-3107W, Sandia National Laboratories Unclassified Unlimited Release (UUR), 2015.
18. **NWTC Information Portal (OpenFAST).** 14-June-2016; Available from: https://nwtc.nrel.gov/OpenFAST.
19. **Horváth, Z.L. and Z. Bor,** *Focusing of truncated Gaussian beams.* Optics communications, 2003. **222**(1-6): p. 51-68.
20. **Carbajo Fuertes, Fernando, and Fernando Porté-Agel.** "Using a virtual Lidar approach to assess the accuracy of the volumetric reconstruction of a wind turbine wake." Remote Sensing 10.5 (2018): 721.
21. **Sirovich, Lawrence**. "Turbulence and the dynamics of coherent structures. I. Coherent structures." Quarterly of applied mathematics 45.3 (1987): 561-571.
22. **Glauser, M.N. and W.K. George**, *Application of multipoint measurements for flow characterization.* Experimental Thermal and Fluid Science, 1992. **5**(5): p. 617-632.
23. **Newman, A.J., D.A. Drew, and L. Castillo,** *Pseudo spectral analysis of the energy entrainment in a scaled down wind farm.* Renewable energy, 2014. **70**: p. 129-141.
24. **Angelou, N., et al.,** *Direct measurement of the spectral transfer function of a laser based anemometer.* Review of scientific instruments, 2012. **83**(3): p. 033111.

Backup Slides

Results – Flow Structure

Convergence of proper orthogonal decomposition calculation

- All cases are converged by at least 1800 s, where convergence is defined when $E(N)$<0.02 (see also Newman *et al.* [23]):

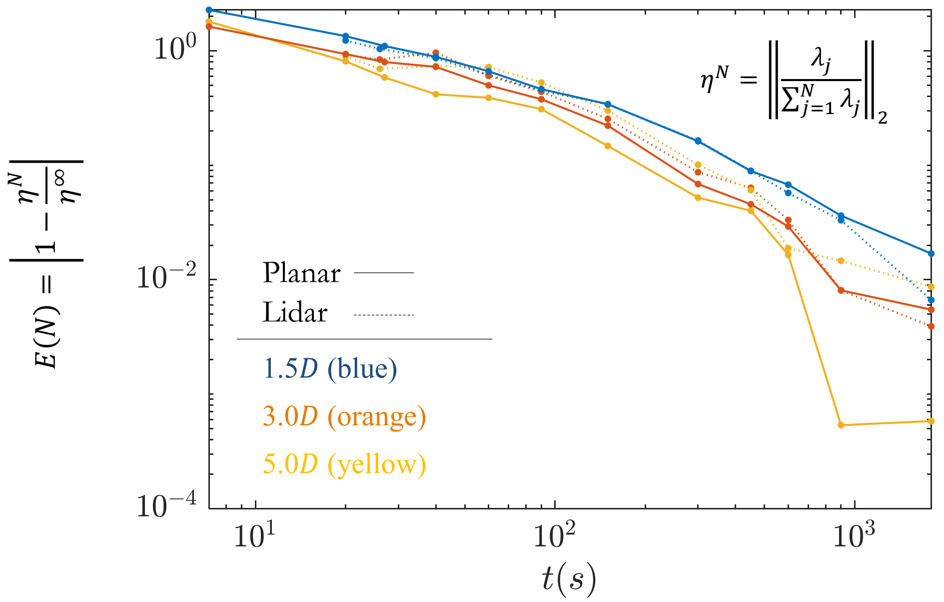

η^N – normalized TKE represented in the modes (λ_j is eigenvalue corresponding to the j^{th} mode and represents the mean TKE of the mode)

N – number of frames used in the decomposition ($N = \infty$ corresponds to the highest frame count available, which is 3600 for the planar data and 1800 for the lidar data)

- Note that any incomplete convergence of the snapshots is manifested in both the planar data and the lidar data, so any potential nonconvergence does not preclude a useful comparative analysis